Performance analysis of the 4DOF vehicle model suspension system under dynamic conditions by design LQR controller for passenger car application

Walelign Wudu Bezabh*, *Ayitenew Mogninet Getaneh*

Department of Mechanical engineering, College of Engineering and Technology, Mizan Teppi University, Teppi, Ethiopia

*Corresponding Author: Email: walelign@mtu.edu.et, walewudu10@gmail.com

Abstract

Designing innovative vehicle systems is a rapidly growing profession in which researchers are interested. However, the ever-increasing improvement requirements for drive dynamics, ride comfort, and vehicle handling provide a challenge. The mathematical modeling of a 4 degree of freedom(DOF) half car model active suspension system (ASS) employing linear quadratic regulator(LQR) controller based on a control Algorithm for ride quality and vehicle handling has been proposed in this study. To simulate the work, MATLAB/Simulink software is employed. The sprung masses of the vehicle's body heave, pitching displacements, and unsprung masses of the wheels heave displacements are the regulated parameters. Its performance is compared to that of the passive suspension system it replaces (PSS). For simulation, two bump sinusoidal roads inputs and a random road type input are employed. From simulation in the vertical direction, the ASS with LQR controller improves performance by 64 percent peak to peak. And also, sprung masses tilting in the lateral direction improved by 67.4 percent. Unsprung masses are simulated under two bump road input disturbances at the front and rear wheel for vehicle handling 51.497 and 40.19 percent peak to peak value, respectively, as opposed to PSS. Finally, the proposed controller's performance was demonstrated in a simulation exercise. The simulation results demonstrates that good modeling and control capabilities have been built in this study.

Index Terms— Active suspension, LQR, 4 DOF, MATLAB/Simulink.

1. Introduction

Designing new vehicle systems is a rapidly expanding profession that attracts the attention of the researchers. The ever-increasing improvement needs relating to drive dynamics, ride comfort, and vehicle handling, however, pose a difficulty. Environmental protection and fuel efficiency have also become major considerations for customers when purchasing a new vehicle. These requirements can be met by developing more effective drive dynamics control mechanisms, such as active suspension systems. The basic purpose of the suspension system is to isolate a vehicle body from road irregularities during braking, cornering and acceleration to improve driving comfort, safety and retain continuous road wheel contact to provide road holding [1, 2, 3]. The term "vehicle handling

regulation" refers to preventing suspension movements from causing insufficient tire-to-road contact. A suspension system is a combination of springs, dampers, and linkages that is responsible for the connection between a vehicle's body and its wheels [4]. The spring carries the body mass by storing energy and helps to isolate the body from road disturbances, while the damper dissipates this energy and helps to damp the oscillations. The vehicle classification most works commonly list the three fundamental varieties of damping suspension systems, namely a passive suspension system (PSS), a semi-active suspension system (SASS), and an active suspension system (ASS) [5,6]. The passive suspension systems suspension is the least complex system and has numerous advantages. But, the disadvantage of passive suspension is the limits of overcoming unwanted vibration that occurs due to road abnormalities [7, 8]. Thus, to achieve better performance results, semi-active suspension uses the conventional spring and externally controlled damper [9]. In contrast to passive systems, active suspension systems can adjust their dynamic characteristics in response to varying road conditions in real-time and offer superior handling, road feel, and responsiveness, as well as roll stability and safety through uses actuators force .The actuator force provides adequate control force to the system based on the input from the various sensors associated with it. Firstly, nowadays, suspension is the main concern, chiefly in automotive applications. However, people do not feel good during transportation. The life of vehicles is also not long because of the limited damping capability of a vehicle suspension system. The customer also blames the manufacturer for the suspension, which easily transfers vibrations to passengers. Secondly, researchers conducted a study on vehicle suspension systems, but most of the work was on the quarter-car model. This is a one-wheel dynamic analysis. So, to overcome these problems in this dissertation study, a complete mathematical model is developed, and then a two-controller with an actuator is designed. Performance analysis was performed to show the significant improvement of the new design. In fact, many independent suspension studies have focused on simpler two-degree-of-freedom quarter car models, with only a few studies focusing on the overall motion control of a half vehicle. Even though a few studies have been done on full dynamic control of the vehicle recently, the built controllers lacked robustness to changes in system parameters [8, 11]. The aim of the automobile suspension system is to not only isolate the influence of road surface disturbances on passengers in order to increase ride comfort, but also to regulate the dynamic tire load with adequate suspension working space in order to improve the vehicle's stability and

safety.. Therefore to overcome the above problems this work gave attention to the half dynamic model of a vehicle and controller design to enhance the active suspension system performance. So, a selected car model includes sprung and unsprung mass dynamics suspension system is developed, and a controllers are designed.

2. Mathematical modelling

For a comparison purpose in this section, a complete mathematical model both active and passive of vehicle model suspension system are derived. So, using Newton's second law of motion, the mathematical equation of vehicle model under a dynamic condition are derived in the next section .for the numerical purpose the selected model are described in the table below

Table1: The parameters characterizing the model are:

Model	Measuring	Numerical
m_S : Vehicle body sprung mass	K g	1794.4
m_{uf} : Unsprung mass at front vehicle body	K g	87.15
m_{ur} : Unsprung mass at rear vehicle body	K g	140.14
c_{sf} : Front suspension damper co-efficient	Ns/m	1190
c_{sr} : Rear suspension damper coefficient	Ns/m	1000
k_{sf} : Stiffness co-efficient at front suspension	N/m	66824
k_{sr} : Stiffness co-efficient at Rear suspension	N/m	18615
k_{uf} : Stiffness co-efficient at front wheel	N/m	101115
k_{ur} : Stiffness co-efficient at rear wheel	N/m	101115
J_S : Pitch Axis Moment of Inertia	K g m^2	3443.05
L_1 : Length between rear wheel and center of gravity	M	1.72
L_2 : Length between front wheel and center of gravity	M	1.27
U_1: Front actuator input		—
U_2 : Rear actuator input		—

Table 2: The variables describing the model are:

Model	Measuring Unit
x_S : Chassis vertical positions at center of gravity	M
x_{Sf} : Front chassis vertical positions	M
x_{sr} : rear chassis vertical positions	M
x_{uf} : Front wheels vertical positions	M
x_{ur}: Rear wheels vertical positions	M
x_{wf} : Front road profiles	m
x_{wr} : Rear road profiles	m

2.1. Mathematical modeling of passive suspension system (PSS)

The mathematical modeling of a linear half-car suspension system with 3 DOFs. In this section, the model is derived along with both vertical and lateral directions. Using Newton's second law of motion, the vehicle dynamic equations of motions under different driving conditions are driven as follows.
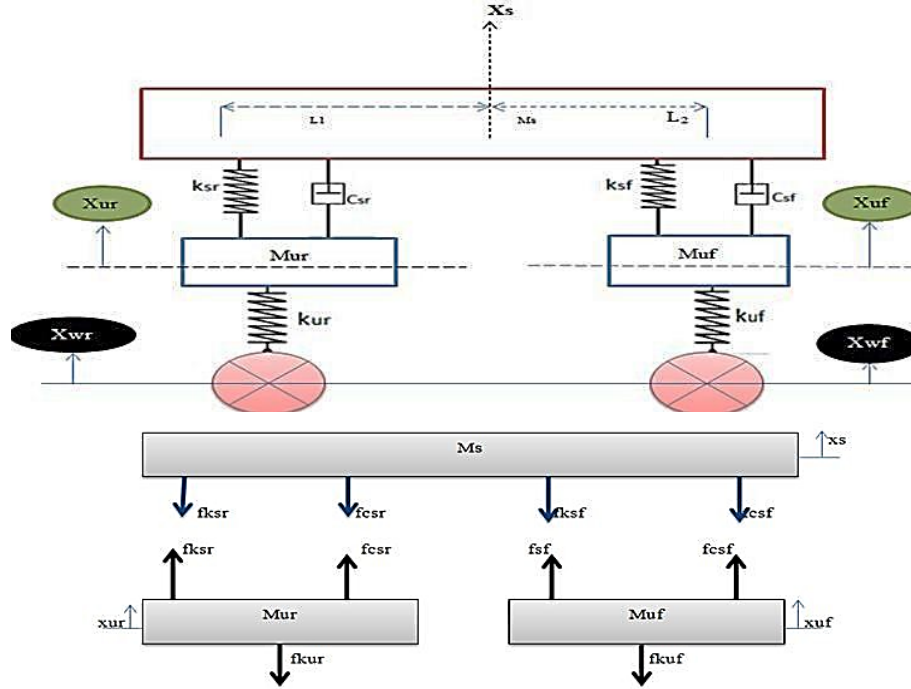

Figure 1: Model a two-wheel passive suspension Figure 2: FBD of 3DOF sprung, unsprung mass at front and rear wheels respectively

The vehicle body bounce motion

$$m_s \ddot{x}_s + c_{sf}\left(\dot{x}_{sf} - \dot{x}_{uf} - L_2\dot{\theta}\right) + k_{sf}\left(x_{sf} - x_{uf} - L_2\theta\right) + c_{sr}\left(\dot{x}_{sr} - \dot{x}_{ur} + L_1\dot{\theta}\right)$$
$$+ k_{sr}\left(x_{sr} - x_{ur} + L_1\theta\right) = 0$$

(1)

The vehicle body bounce motion at front wheel

$$m_{uf}\, x_{uf} - c_{sf}\left(\dot{x}_{sf} - \dot{x}_{uf} - L_2\dot{\theta}\right) - k_{sf}\left(x_{sf} - x_{uf} - L_2\theta\right) + k_{uf}\left(x_{uf} - x_{wf}\right) = 0 \qquad (2)$$

The vehicle body bounce motion at rear wheel

$$m_{ur}\ddot{x}_{ur} - c_{sf}\left(\dot{x}_{sr} - \dot{x}_{ur} + L_1\dot{\theta}\right) - k_{sr}\left(x_{sr} - x_{ur} + L_1\theta\right) + k_{ur}\left(x_{ur} - x_{wr}\right) = 0 \qquad (3)$$

Mathematical model for a vehicle body pitching motion

$$J\ddot{\theta} - L_2 c_{sf}\left(\dot{x}_{sf} - \dot{x}_{uf} - L_2\dot{\theta}\right) - L_2 k_{sf}\left(x_{sf} - x_{uf} - L_2\theta\right) + L_1 c_{sr}\left(\dot{x}_{sr} - \dot{x}_{ur} + L_1\dot{\theta}\right)$$
$$+ L_1 k_{sr}\left(x_{sr} - x_{ur} + L_1\theta\right) = 0 \tag{4}$$

2.2. Mathematical modeling of Active suspension system (ASS)

The state variable in active suspension system can control through a controller which are selected for this study.
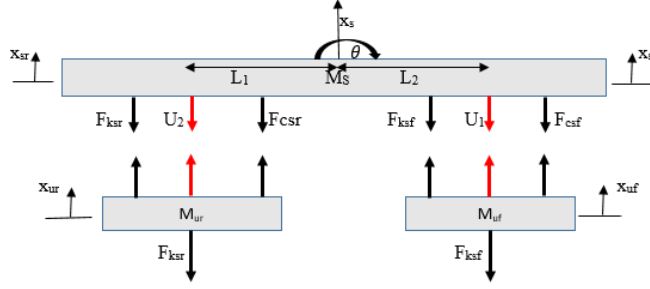

Figure 3: FBD of 4DOF sprung, unsprung mass at front and rear wheel respectively

The model equation of a sprung mass on vertical motion at center gravity point

$$m_s\ddot{x}_s + c_{sf}\left(\dot{x}_{sf} - \dot{x}_{uf} - L_2\dot{\theta}\right) + k_{sf}\left(x_{sf} - x_{uf} - L_2\theta\right) + c_{sr}\left(\dot{x}_{sr} - \dot{x}_{ur} + L_1\dot{\theta}\right)$$
$$+ k_{sr}\left(x_{sr} - x_{ur} + L_1\theta\right) + F_{AF} + F_{AR} = 0 \tag{5}$$

$$\ddot{x}_s = \cfrac{-\left[\begin{array}{l} c_{sf}\left(\dot{x}_{sf} - \dot{x}_{uf} - L_2\dot{\theta}\right) + k_{sf}\left(x_{sf} - x_{uf} - L_2\theta\right) + c_{sr}\left(\dot{x}_{sr} - \dot{x}_{ur} + L_1\dot{\theta}\right) \\ + k_{sr}\left(x_{sr} - x_{ur} + L_1\theta\right) - F_{AF} - F_{AR} \end{array}\right]}{m_s} \tag{6}$$

$$J\ddot{\theta} - L_2 c_{sf}\left(\dot{x}_{sf} - \dot{x}_{uf} - L_2\dot{\theta}\right) - L_2 k_{sf}\left(x_{sf} - x_{uf} - L_2\theta\right) + L_1 c_{sr}\left(\dot{x}_{sr} - \dot{x}_{ur} + L_1\dot{\theta}\right)$$
$$+ L_1 k_{sr}\left(x_{sr} - x_{ur} + L_1\theta\right) - L_2 F_{AF} + L_1 F_{AR} = 0 \tag{7}$$

$$\ddot{\theta} = \cfrac{\left[\begin{array}{l} L_2 c_{sf}\left(\dot{x}_{sf} - \dot{x}_{uf} - L_2\dot{\theta}\right) + L_2 k_{sf}\left(x_{sf} - x_{uf} - L_2\theta\right) - L_1 c_{sr}\left(\dot{x}_{sr} - \dot{x}_{ur} + L_1\dot{\theta}\right) \\ - L_1 k_{sr}\left(x_{sr} - x_{ur} + L_1\theta\right) + L_2 F_{AF} - L_1 F_{AR} \end{array}\right]}{J} \tag{8}$$

$$m_{ur}\ddot{x}_{ur} - c_{sr}\left(\dot{x}_{sr} - \dot{x}_{ur} + L_1\dot{\theta}\right) - k_{sr}\left(x_{sr} - x_{ur} + L_1\theta\right) + k_{ur}\left(x_{ur} - x_{wr}\right) + F_{AR} = 0 \tag{9}$$

$$\ddot{x}_{ur} = \cfrac{\left[c_{sr}\left(\dot{x}_{sr} - \dot{x}_{ur} + L_1\dot{\theta}\right) + k_{sr}\left(x_{sr} - x_{ur} + L_1\theta\right) - k_{ur}\left(x_{ur} - x_{wr}\right) - F_{AR}\right]}{m_{ur}} \tag{10}$$

$$m_{uf}\ddot{x}_{uf} - c_{sf}\left(\dot{x}_{sf} - \dot{x}_{uf} + L_2\dot{\theta}\right) - k_{sf}\left(x_{sf} - x_{uf} + L_2\theta\right) + k_{ur}\left(x_{uf} - x_{wf}\right) + F_{Af} = 0 \tag{11}$$

$$\ddot{x}_{uf} = \cfrac{\left[c_{sf}\left(\dot{x}_{sf} - \dot{x}_{uf} + L_2\dot{\theta}\right) + k_{sf}\left(x_{sf} - x_{uf} + L_2\theta\right) - k_{uf}\left(x_{uf} - x_{wf}\right) - F_{Af}\right]}{m_{uf}} \tag{12}$$

For a control purpose the state variable should be linear independent
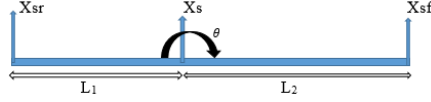
Assume that the pitching dynamics to forward direction is positive

$$\theta = \frac{x_{sr} - x_{sf}}{L}, \qquad x_s = \frac{L_2 x_{sr} + L_1 x_{sf}}{L}$$

2.2.1. State space model for active suspension system

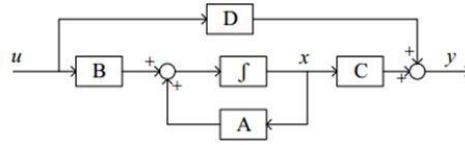The model can be written in the following state space form

Figure 4: Block diagram for state space representation

$$\dot{x}(t) = Ax(t) + BU$$
$$y = Cx(t) + DU$$

(13)

Let

$$x_{sr} = x_1, \dot{x}_{sr} = x_2, x_{ur} = x_3, \dot{x}_{ur} = x_4, x_{sf} = x_5, \dot{x}_{sf} = x_6, x_{uf} = x_7, \dot{x}_{uf} = x_8$$

$$y_1 = \frac{L_2 + L}{L}, y_2 = \frac{L_1 + L}{L}, y_3 = \frac{L_2}{L}, y_4 = \frac{L_1}{L}, z_4 = \frac{L^2{}_1 m_s + j}{m_s j}$$

$$z_1 = \frac{L_1 L_2 m_s - J - L L_2 m_s}{m_s}, z_2 = \frac{L_1 m_s L - L^2{}_1 m_s - j}{m_s j},$$

$$z_3 = \frac{L_1 L_2 m_s - j}{m_s j}, z_4 = \frac{L_1{}^2 m_s + j}{m_s j}$$

$$\dot{x}_2 = z_3 \begin{pmatrix} c_{sf}\left(y_1 x_6 - y_3 x_2 - x_8\right) \\ + k_{sf}\left(y_1 x_5 - y_3 x_1 - x_7\right) \end{pmatrix} - z_4 \begin{pmatrix} c_{sr}\left(y_2 x_2 - y_4 x_6 - x_4\right) \\ + k_{sr}\left(y_2 x_1 - y_4 x_5 - x_3\right) \end{pmatrix} + z_3 u_1 - z_4 u_2 \qquad (14)$$

$$\dot{x}_4 = \frac{c_{sr}\left(y_2 x_2 - y_4 x_6 - x_4\right) + k_{sr}\left(y_2 x_1 - y_4 x_5 - x_3\right) - k_{ur}\left(x_3 - x_{wr}\right) - u_2}{m_{ur}} \qquad (15)$$

$$\dot{x}_6 = z_1 \begin{pmatrix} c_{sf}\left(y_1 x_6 - y_3 x_2 - x_8\right) \\ + k_{sf}\left(y_1 x_5 - y_3 x_1 - x_7\right) \end{pmatrix} + z_2 \begin{pmatrix} c_{sr}\left(y_2 x_2 - y_4 x_6 - x_4\right) \\ + k_{sr}\left(y_2 x_1 - y_4 x_5 - x_3\right) \end{pmatrix} + z_1 u_1 - z_2 u_2 \qquad (16)$$

$$\dot{x}_8 = \frac{c_{sf}\left(y_1 x_6 - y_3 x_2 - x_8\right) + k_{sf}\left(y_1 x_5 - y_3 x_1 - x_7\right) - k_{uf}\left(x_7 - x_{wf}\right) - u_1}{m_{uf}}$$

(17)

The value of the feedback controller vector U is defined as U (t) = -Kx. The state feedback gain matrix, K, can be calculated in different ways. In this study, the optimal value K is obtained from the inbuilt Matlab command K = lqr (A; B; Q; R).

Based on the physical model of the vehicle in Fig.5 the state space equations of the suspension system for design purpose of the LQR control are as:

Let

$$\lfloor A_1\rfloor = \begin{bmatrix} 0 & 1 & 0 & 0 & 0 & 0 & 0 & 0 \end{bmatrix}, \ \lfloor A_3\rfloor = \begin{bmatrix} 0 & 0 & 0 & 1 & 0 & 0 & 0 & 0 \end{bmatrix}, \ \lfloor A_5\rfloor = \begin{bmatrix} 0 & 0 & 0 & 0 & 0 & 1 & 0 & 0 \end{bmatrix}$$

$$\lfloor A_7\rfloor = \begin{bmatrix} 0 & 0 & 0 & 0 & 0 & 0 & 0 & 1 \end{bmatrix}, \ [A_4] = \begin{bmatrix} \dfrac{y_2{}^*k_{sr}}{m_{ur}} & \dfrac{y_2{}^*c_{sr}}{m_{ur}} & \dfrac{-k_{sr}-k_{ur}}{m_{ur}} & \dfrac{-c_{sr}}{m_{ur}} & \dfrac{-y_4{}^*k_{sr}}{m_{ur}} & \dfrac{-y_4{}^*c_{sr}}{m_{ur}} & 0 & 0 \end{bmatrix}$$

$$[A_8] = \begin{bmatrix} \dfrac{-y_3{}^*k_{sf}}{m_{uf}} & \dfrac{-y_3{}^*c_{sf}}{m_{uf}} & 0 & 0 & \dfrac{y_1{}^*k_{sf}}{m_{uf}} & \dfrac{y_1{}^*c_{sf}}{m_{uf}} & \dfrac{-k_{sf}-k_{uf}}{m_{uf}} & \dfrac{-c_{sf}}{m_{uf}} \end{bmatrix}$$

$$[A_2] = \begin{bmatrix} -z_3{}^*k_{sf}{}^*y_3 - z_4{}^*k_{sr}{}^*y_2 \\ -z_3{}^*c_{sf}{}^*y_3 - z_4{}^*c_{sr}{}^*y_2 \\ z_4{}^*k_{sr} \\ z_4{}^*c_{sr} \\ z_3{}^*k_{sf}{}^*y_1 + z_4{}^*k_{sr}{}^*y_4 \\ z_3{}^*c_{sf}{}^*y_1 + z_4{}^*c_{sr}{}^*y_4 \\ -z_3{}^*k_{sf} \\ -z_3{}^*c_{sf} \end{bmatrix}^T, \quad [A_6] = \begin{bmatrix} z_2{}^*k_{sr}{}^*y_2 - z_1{}^*k_{sf}{}^*y_3 \\ z_2{}^*c_{sr}{}^*y_2 - z_1{}^*c_{sf}{}^*y_3 \\ -z_2{}^*k_{sr} \\ -z_2{}^*c_{sr} \\ z_1{}^*k_{sf}{}^*y_1 - z_4{}^*k_{sr}{}^*y_4 \\ z_1{}^*c_{sf}{}^*y_1 - z_2{}^*c_{sr}{}^*y_4 \\ -z_1{}^*k_{sf} \\ -z_1{}^*c_{sf} \end{bmatrix}^T, \quad [G] = \begin{bmatrix} u_1 & u_2 \end{bmatrix}^T$$

$$[B] = \begin{bmatrix} 0 & z_3 & 0 & 0 & 0 & z_1 & 0 & -1/m_{uf} \\ 0 & -z_4 & 0 & -1/m_{ur} & 0 & -z_2 & 0 & 0 \end{bmatrix}^T, \quad [G] = \begin{bmatrix} 0 & 0 & 0 & 0 & 0 & 0 & 0 & k_{uf}/m_{uf} \\ 0 & 0 & 0 & k_{ur}/m_{ur} & 0 & 0 & 0 & 0 \end{bmatrix}^T$$

3. Control system design

The objective of any control system is to sense the deviation of the output from the desired value and then correct it, till the desired output is achieved. In this paper, the LQR controller is applied based on its design requirements. However, the accuracy of the entire

system depends on how sensitive the controller is to the error detected and how it is manipulated into error.

3.1. LQR controller

The linear quadratic regulator is a special type of optimal control problem that deals with linear mechanism and the minimization of cost or objective functions that are quadratic in state and in control (subject to some constraints) with performance index determination [10]. In this study, the linear quadratic regulator controller is used to improve both ride comfort by minimizing the error between sprung and unsprung mass and vehicle handling by minimizing the error on unsprung mass reference to the ground. The objective of optimal control is to determine a control vector (U_1 and U_2) that forces the behavior of the dynamic system to the required final state by minimizing the cost of function and also, at the same time, fulfilling the physical constraints.

From Eq. (13) the state variable feedback regulator is determined using the following equation: $U_{(LQR)(t)} = -K_{x(t)}$, where K is the state feedback gain matrix.

$$J = \int_{0}^{\infty} \left(x^T Q_x + U^T R U \right) dt \tag{18}$$

• The system must be completely state controllable

• R must be positive definite

• The system must be observable
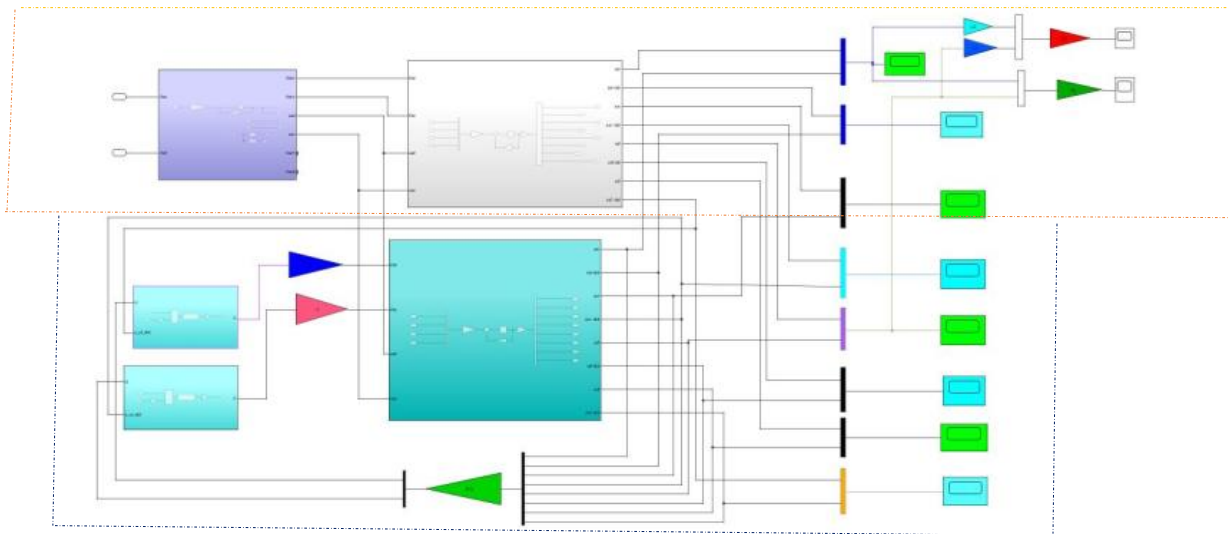
• Q must be semi-positive definite

Figure5. Block diagram of LQR controller for half car model

The above Figure 5 show that the half car 4 DOF active suspension system model and control systems have been developed using MATLAB Simulink tool. In Figure 5 the above section show the Simulink model for passive suspension model and the below section show that half car model active suspension system with LQR control system.

4. Simulation and result analysis

Numerical simulations on the 4 DOF half vehicle model ASS are performed in this section to validate the proposed LQR control's control performance. The vehicle parameters are listed in Table 1 for simulation purposes. Matlab/Simulink software is used to run the simulation.

4.1. Comparative performance of ASS to PSS simulation for two bump Sinusoidal road input

For this study totally four road inputs have taken as a disturbance. The first two types are sinusoidal function which are expected input type and the other two are random type road inputs with the selected vehicle speed (at 20, 40, 60 and 80km/hr).These simulations are used to test the effectiveness of the ASS over the PSS on two different bump road profiles. The two bump sinusoidal road profiles are shown below, with h denoting the bump amplitude and 0.005m as the value [9, 13]. Two bumps were identified in a sinusoidal bump with a frequency of 8 HZ. The input of sinusoidal highways with a frequency of 8 HZ has been described as follows:

$$x_{wf(t)} = \begin{cases} h(1-\cos(8\pi t)), 0.5 \leq t \leq 0.75\sec \\ h\left(\dfrac{1-\cos(8\pi t)}{2}\right), 3.5 \leq t \leq 3.75\sec \\ 0, otherwise \end{cases} \text{ And } x_{wr(t)} = \begin{cases} h(1-\cos(8\pi t)), 3 \leq t \leq 3.25\sec \\ h\left(\dfrac{1-\cos(8\pi t)}{2}\right), 7.25 \leq t \leq 7.5\sec \\ 0, otherwise \end{cases} \quad (19)$$

An input disturbance for the front wheel and an input disturbance for the rear wheel are Eq.19
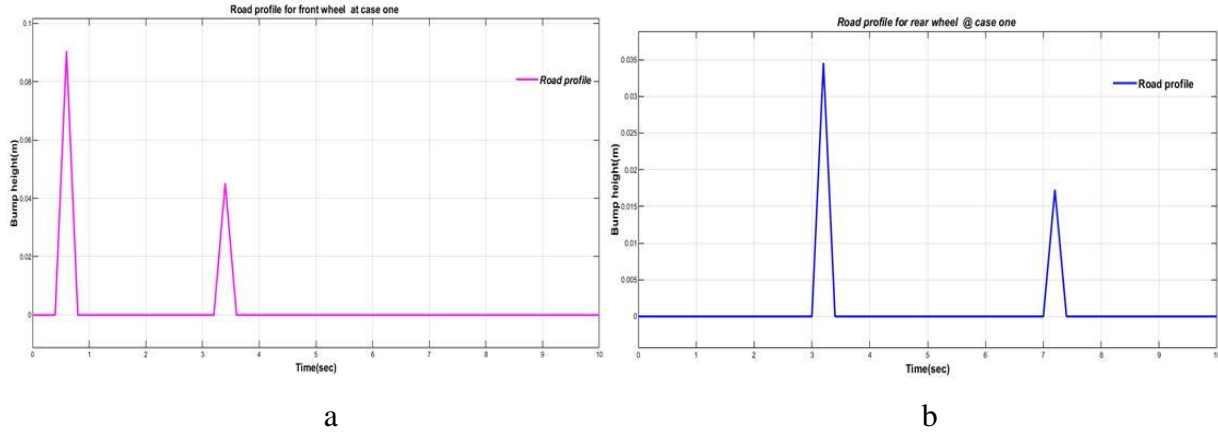
a	b

Figure6: Front wheel and Rear wheel two bump expected road profile simulation

Based on ISO, provides the classification of road roughness for this study. As described below the random type B (good) and type C (average) type of road inputs are designed at four-vehicle operating speeds. These are; (20km/hr,40km/hr,60km/hr,80 km/hr) which helps to show the effects of road roughness and the vehicle speeds in addition to the improvement of road handling and ride quality for passengers. The power spectral density at each vehicle speeds are calculated with Eq20.

$$x_{w(t)} = \sqrt{k} \int w(t)dt \qquad (20)$$

Where v is the vehicle speed, w (t) white noise, k is the spectral density constant, $k = 4\pi^2 n_o^2 G(n_o)v$

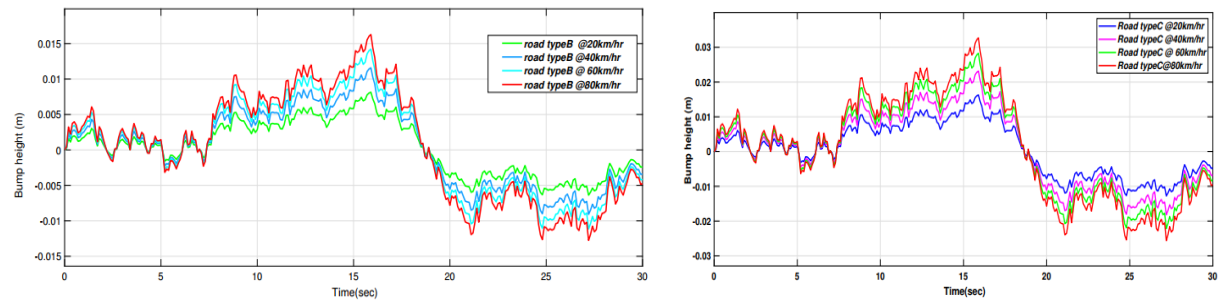G (no) value for B and C type road input $=16 * 10^{-6}m^3, 64 * 10^{-6}m^3$ respectively. [12]

Figure 7: Random road profile type B, and C at selected vehicle speed simulated respectively.

4.1.1. Sprung mass displacements

The comparison of ASS and PSS performance for the parameters of vehicle body heave and pitch displacements is shown in the figures below. PSS has a substantially higher peak to peak amplitude displacement than ASS in all states of the system, as shown in the simulation graph. The performance of ASS and PSS was compared in terms of peak to peak displacement and

settling time. All regulated ASS states outperform uncontrolled PSS states by more than 40% in terms of peak to peak and settling time, which are great results.
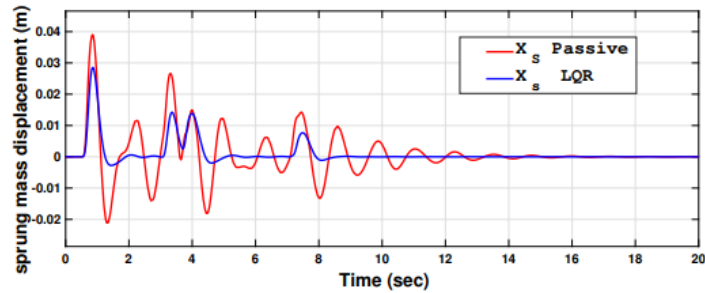

Figure 8: The chassis position at center of gravity.

Figure 8. Shows the chassis location in both the passive and active systems with LQR. The new model with a controller makes a substantial contribution by minimizing error and enhancing ride comfort, as illustrated in the figure showing the displacement of the sprung mass at the center of gravity. The peak to peak value of the vehicle body's suspension travel is 0.031 m, compared to 0.06 m for the passive value. Beyond that, the controller responds quickly, and the system stabilizes rather than continuing to vibrate.
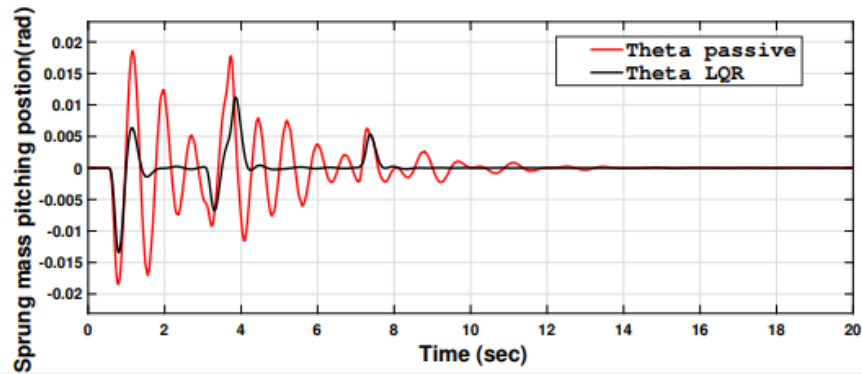

Figure 9: Sprung mass pitching dynamics at center of gravity.

The half-car pitching dynamics condition for a 20-second period with forecasted bump inputs. The peak value is lowered from 0.018 to 0.0058 rad in the simulated figure. The negative peak, on the other hand, is -0.017 without a controller and -0.013 with one.
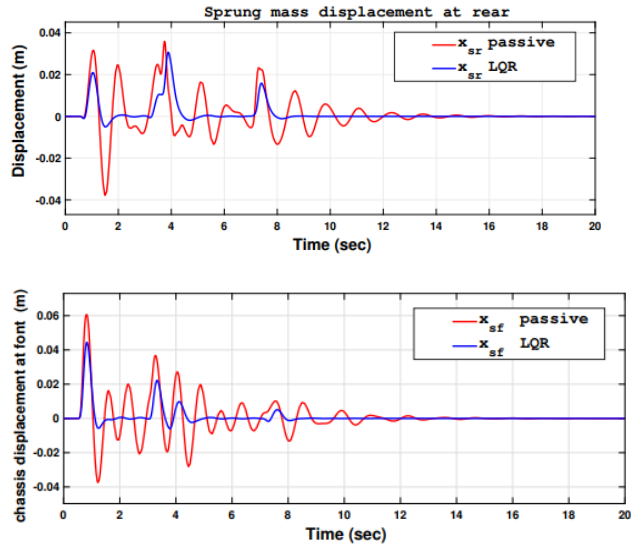
Figure 10: The chassis position at rear and sprung mass displacement at front respectively.

4.1.2. Unsprung mass displacements

The performance of ASS and PSS for the parameters of front wheel heave and rear wheel heave displacements is shown in Fig 12 and 13. The peak to peak amplitude displacement for PSS is substantially larger than ASS for all states of the system, as seen in the simulation graph. The performance of ASS and PSS was compared on the basis of peak to peak displacement and settling time. All regulated ASS states have a peak to peak and settling monitoring processes of more than 44.83% over uncontrolled PSS states, which are exceptional results. Tables3 provide the details of their peak to peak values and settling times, respectively.
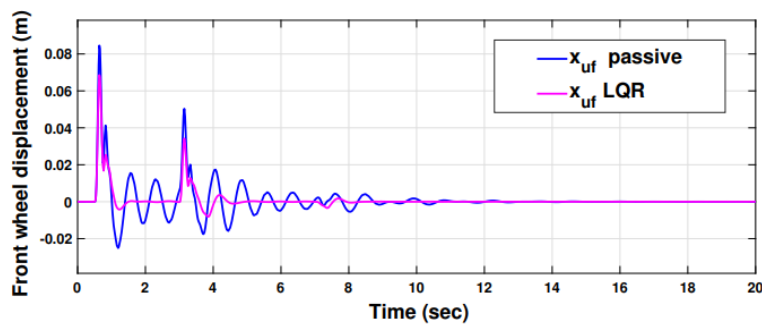

Figure 12: Front wheel heave displacement simulation.

Figure 12 shows the displacement of the active suspension system with the LQR controller compared with the passive. It is observed that the active suspension system with an LQR

controller gives a minimum bump height value as compared with the conventional damping system at the same road disturbance inputs. It is clear that the suspension system with the controller became stable due to the actuator force which is generated based on the feedback through the control system.
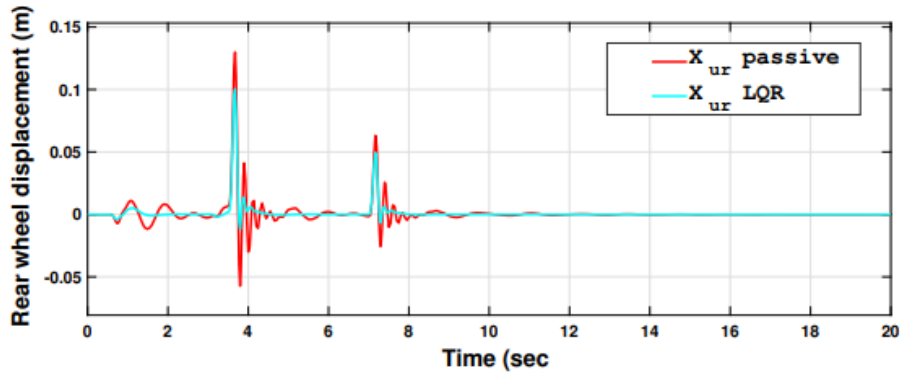

Figure 13: Rear wheel heave displacement simulation.

As mentioned in the simulated figures, results from the Matlab/ Simulink are comparison of the suspension models passive and active with the LQR controller .The parameter for the study are the same as it mentioned in Table1. The result tells us the new model (suspension with LQR) controller improves both the ride and vehicle handling at each case road inputs. Peak- to -Peak Value: the peak to peak value is the vertical distance between the top and bottom of the wave. It is measured in suspension parameters and may be labeled V_{pp}

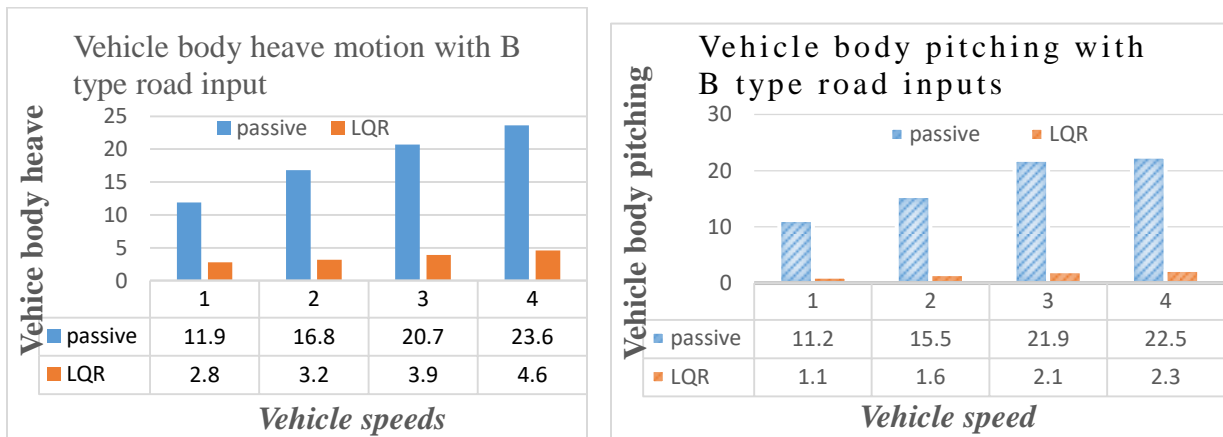$$Im\,provment = \frac{Passive\,value - Active\,value}{Passive\,value}$$

(21)

Table 3: Comparison of peak to peak displacement and settling time system with LQR controller to previous work simulations

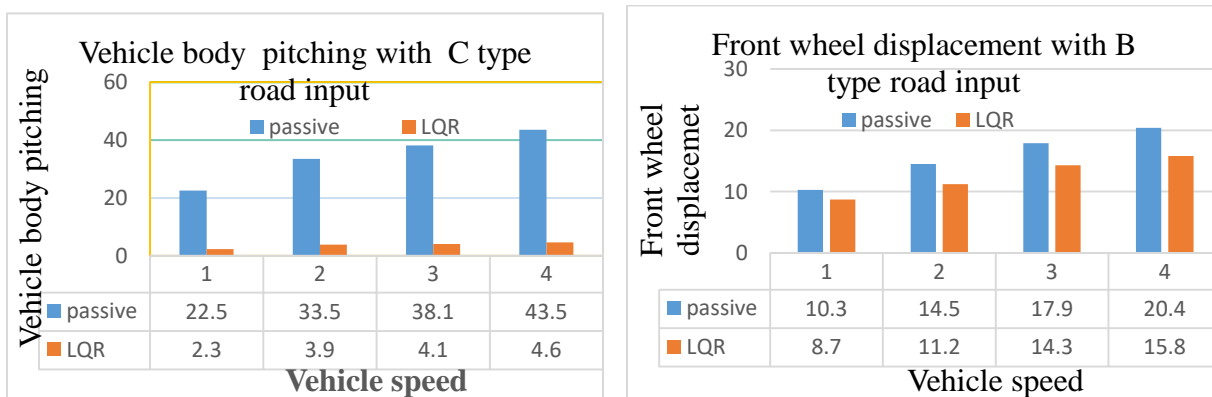| Parameters	P to P Passive	P to P LQR	Passive(sec)	LQR(sec)	Improvement %	
					Settling time	P to P
Vehicle's body heave	0.06036	0.02220	16	8	50	63.214
Vehicle's body pitch	0.03901	0.01272	14.5	7.8	46.2	67.400
Vehicle's body heave at front	0.09825	0.03629	16.3	8	51	63.056
Vehicle's body heave at rear	0.07333	0.02593	16	8	50	64.638
Front wheel heave	0.11028	0.05349	14.4	7.6	47.22	51.497
Rear wheel heave	0.18722	0.11197	14.5	8	44.83	40.194

4.2. Simulation results the model on Band C type random road input at 20, 40, 60, and 80 km/hr vehicle speeds

The performance comparison of PSS to active suspension system with LQR controller has been simulated when traversing at vehicle speeds of 20 km/hr, 40 km/hr, 60 km/hr, and 80 km/hr for the states of, vehicle's body (chassis) heave at the center of gravity, front-wheel displacement, rear-wheel displacement, and pitch displacements on B and C class random road input. The graph shows the relation between the road input and vehicle speed simulation is simulated in this section.

Vehicle body heave motion with B type road input

	1	2	3	4
passive	11.9	16.8	20.7	23.6
LQR	2.8	3.2	3.9	4.6

Vehicle speeds

Vehicle body pitching with B type road inputs

	1	2	3	4
passive	11.2	15.5	21.9	22.5
LQR	1.1	1.6	2.1	2.3

Vehicle speed

Graph1 show the vehicle body heave and pitching dynamics with B type road input

Graph 1, it is easy to know that these performance indicators are sensitive to the road surface. Compared with the passive suspension, the RMS values of the system with a controller are reduced by the high-value difference. At all values of vehicle speed, the RMS value is greatly improved in the new design.

Vehicle body pitching with C type road input

	1	2	3	4
passive	22.5	33.5	38.1	43.5
LQR	2.3	3.9	4.1	4.6

Vehicle speed

Front wheel displacement with B type road input

	1	2	3	4
passive	10.3	14.5	17.9	20.4
LQR	8.7	11.2	14.3	15.8

Vehicle speed

Graph2 show the vehicle body pitching and front wheel displacement with C and B type road input

As the simulation results illustrate, the peak-to-peak amplitude for PSS is much larger than the ASS for all states. The comparative performance of ASS to PSS is also demonstrated under peak-to-peak displacement and settling time values. Their detailed peak-to-peak values are given in Table 3 which shows the improvement of the suspension with the LQR controller and how much it reduces the settling time and peak-to-peak value. Two road bumps are exerted on the rear and front tires with lag time between the two wheels. The active system model with the controller shows amplitude values. And also, the figure depicts that the settling time in LQR is attenuated in the controllers. The control mechanism provides a good settling time reduction.

5. Conclusion

The modeling and control of a vehicle suspension system for a passenger half car is covered in this study. Under a dynamical condition, a mathematical model for linear 4 DOF vehicle model suspensions systems has been constructed and derived. Following the creation of the dynamic model, a selected controller is applied, and its performance is assessed at various vehicle speeds under bump road input disturbances.

A simulation using MATLAB/Simulink is used to validate the controller's performance and efficiency. The controller's job is to bring a vehicle's motions to a state of equilibrium with a minimal amplitude and quick settle time. For example, sprung mass heave displacement in the lateral direction is 67.4 percent, 63.214 percent in the vertical direction, and the peak to peak amplitude displacement for PSS and ASS is 0.06036 m and 0.02220 m, respectively. The percentage reduction of ASS to PSS during the settling time at a minimum 44.83 % with to each vehicle suspension parameter. As a result, the results reveal that the developed controller increases ride comfort and vehicle handling significantly. The findings shows that in controlled ASS, the amplitude and settling time of sprung and unsprung masses heave displacements are significantly lower than in uncontrolled PSS. Overall, the ASS's dynamic modeling and LQR controller are effective and deliver good results.

Acknowledgements

Reference

[1]. Avesh M, Srivastava R. Modeling simulation and control of active suspension system in Matlab Simulink environment. In2012 Students Conference on Engineering and Systems 2012 Mar 16 (pp. 1-6). IEEE.

[2]. Khan MA, Abid M, Ahmed N, Wadood A, Park H. Nonlinear control design of a half-car model using feedback linearization and an LQR controller. Applied Sciences. 2020 Jan;10(9):3075.

[3] Fischer D, Isermann R. Mechatronic semi-active and active vehicle suspensions. Control engineering practice. 2004 Nov 1;12(11):1353-67.

[4]. Lauwerys C, Swevers J, Sas P. Robust linear control of an active suspension on a quarter car test-rig. Control engineering practice. 2005 May 1;13(5):577-86.

[5]. Chen H, Guo KH. Constrained H/sub/spl infin//control of active suspensions: an LMI approach. IEEE Transactions on Control Systems Technology. 2005 Apr 25;13(3):412-21.

[6].Sharkawy AB. Fuzzy and adaptive fuzzy control for the automobiles' active suspension system. Vehicle system dynamics. 2005 Nov 1;43(11):795-806.

[7].Sun J, Yang Q. Compare and analysis of passive and active suspensions under random road excitation. In2009 IEEE International Conference on Automation and Logistics 2009 Aug 5 (pp. 1577-1580). IEEE.

[8]. Antehunegn Y, Belete M. Control of 8 DOF vehicle model suspension system by designing Second order SMC Controller. GSJ. 2020 Dec;8(12).

[9] Ahmed AE, Ali AS, Ghazaly NM, Abd el-Jaber GT. PID controller of active suspension system for a quarter car model. International Journal of Advances in Engineering & Technology. 2015 Dec 1;8(6):899.

[10]. Ajasa AA, Sebiotimo AA. The use of Matlab in the Solution of Linear Quadratic Regulator (LQR) Problems.

[11]. Naidu DS. Optimal control systems. CRC press; 2002 Aug 27.

[12]. Gandhi P, Adarsh S, Ramachandran KI. Performance analysis of half car suspension model with 4 DOF using PID, LQR, FUZZY and ANFIS controllers. Procedia Computer Science. 2017 Jan 1;115:2-13.

[13]. Hasbullah F, Faris WF. A comparative analysis of LQR and fuzzy logic controller for active suspension using half car model. In2010 11th International Conference on Control Automation Robotics & Vision 2010 Dec 7 (pp. 2415-2420). IEEE.